A Spatio-Spectral Hybrid Convolutional Architecture for Hyperspectral Document Authentication

Muhammad Jaleed Khan[1], Khurram Khurshid[1], Faisal Shafait[2,3]
[1]Artificial Intelligence and Computer Vision (iVision) Lab, Department of Electrical Engineering,
Institute of Space Technology (IST), Islamabad, Pakistan.
[2] School of Electrical Engineering and Computer Science (SEECS),
National University of Sciences and Technology (NUST), Islamabad, Pakistan.
[3] Deep Learning Laboratory, National Center of Artificial Intelligence (NCAI), Islamabad, Pakistan.
Email: faisal.shafait@seecs.edu.pk

***Abstract*—Hyperspectral Document Image (HSDI) analysis allows for efficient and accurate differentiation of inks with visually similar color but unique spectral response, which is a crucial step in authentication of documents. Various HSDI based ink discrimination methods are available in the current literature, however, more accurate and robust methods are required to empower document authentication. Contrary to the former ink mismatch detection methods based on spectral features only, we present a novel method based on deep learning that exploits the spectral correlation as well as the spatial context to enhance ink mismatch detection. Spectral responses of the target pixel and its neighboring pixels are organized in an image format and fed to a Convolutional Neural Network (CNN) for classification. The proposed method achieves the highest accuracy among the other ink mismatch detection methods on the UWA Writing Ink Hyperspectral Images database (WIHSI), which demonstrates the effectiveness of deep learning models employing spatio-spectral hybrid features for document authentication. Detailed experimental analysis for selection of appropriate CNN architecture, spatio-spectral data format and training ratio is presented along with a comparison with the previous methods on this subject.**

Keywords*— Convolutional neural network, deep learning, document analysis, forgery detection, hyperspectral imaging, ink mismatch detection, spatio-spectral hybrid features.

I. INTRODUCTION

Hyperspectral imaging is a state-of-the-art spectral sensing method that provides broad spectral information about the underlying material. Hyperspectral imaging is a widely used technique in remote sensing, art conservation and archeology, artwork authentication, forensic science, image guided surgery and medical diagnosis, crime scene analysis, food quality control, and defense and homeland security [1]. Due to the material identification property of hyperspectral imaging systems, they bear tremendous potential for forensic examination of traces [2], including inks in document images. Easton et al. [3] did the pioneering work in employing hyperspectral imaging for document analysis. Christens-Barry et al. [4] developed EurekaVision, a hyperspectral imaging system for acquisition of Hyperspectral Document Images (HSDIs). Hyperspectral imaging has proved its performance in recovery of degraded scripts [5], dating of manuscripts [6], forensic assessment [2], ink mismatch detection [7], improving readability [8] of documents and response extraction [9]. Deep learning plays an important role in classification problems in hyperspectral image analysis. Convolutional Neural Network (CNN), a state-of-the-art deep learning model for image classification and automatic feature extraction, has evolved as an effective tool for classification of HSIs [10]. Liang et al. [11] proposed classification of hyperspectral data by using sparse representation of deep features extracted by CNN. Leng et al. [12] employed CNN for feature extraction and SVM for pixel classification in hyperspectral images.

Ink mismatch detection is a crucial step in authentication of a questioned document. This document can be a sheet of paper with machine-printed text or handwriting such as a business contract, fraudulent cheque or a ransom note. The presence of one or more inks in minor proportions in a document, apart from the primary ink present in the major proportion, can indicate some fraudulent manipulation made in that document. Several methods for ink mismatch detection based on HSI analysis have been proposed in the last decade to improve and automate document authentication. These methods include k-means clustering [7], localized hyperspectral image analysis [13], fuzzy c-means clustering with feature selection [14], hyperspectral unmixing [15], and deep convolutional network [16]. Deep learning based pixel classification methods in HSIs use only the spectral information [17]. However, spectral responses of the neighboring pixels are eminently correlated to the target pixel, therefore, fusion of both spatial and spectral content provides better high level features without increasing the complexity of the CNN model [12].

In this work, we propose a CNN based ink mismatch detection method for HSDIs that employs a combination of spectral and spatial features of ink pixels for classification. CNN is trained with the spectral responses of segmented ink pixels along with their neighboring pixels formatted in an image form, which is then employed to distinguish between different inks present in questioned documents for authentication. Comprehensive experiments were conducted on mixed ink combinations containing inks from different manufacturers mixed in varying ratios. The proposed method achieves the highest accuracy reported to date (99.6% for blue and 92.3% for black ink) on the publicly available UWA Writing Ink Hyperspectral Images (WIHSI) database [7].

Section II covers the background study, the proposed method is explained in detail in Section III and the experimental results are presented in Section IV followed by the conclusion and future directions in Section V.

II. Background

Document authentication is an increasingly common requirement at many places for various applications. For example, it is needed for cheque verification in banks, degree verification in universities and verification of identification documents in government offices. Over the last few years, researchers have proposed different techniques for document authentication. The latest methods are based on hyperspectral imaging due to its ability to capture useful information content beyond the visible range. Authentication methods for documents involving handwritten notes and signatures are based on ink analysis. The following subsections present the review of HSI based document authentication methods, use of spatio-spectral hybrid features for classification in HSI and deep learning based feature extraction and classification methods.

A. *Document Authentication using HSI Analysis*

The use of HSI analysis in forensic examination has significantly improved the document authentication methods. In order to further improve its performance and practical applicability, several HSI analysis methods for ink discrimination have been proposed during the past decade. Brauns et al. [18] proposed a non-destructive HSI based method for detection of forged documents using an interferometer with frequency tuning and speed adjustment of acquisition. This work provided the necessary proof of concept for HSI based discrimination between writing inks and concluded that unsupervised methods can segregate the ink spectra into different classes. Later on, this work was improved to achieve high spectral and spatial resolution images for analysis of historic documents [19]. Ink-deposition traces [20] and texture [21] information is also useful in handwriting and forensic analysis. Silva et al. [22] deliberated on inks of different ages and introduced a chemo-metric and HSI analysis based document authentication technique. Morales et al. [23] designed a hardware system for analysis of inks using least square SVM classifier and HSI analysis. Qureshi et al. [24] have highlighted the applications of and key challenges involved in acquisition and processing of HSDIs.

Khan et al. [7] collected the WIHSI database using an end-to-end HSI acquisition system and employed k-means clustering for ink mismatch detection in questioned documents assuming that each document comprises equal content of two different inks. Khan et al. [25] presented a combined sparse channel selection technique for selection of discriminative bands from HSDI to ensure accurate ink mismatch detection, and presented solutions for mitigation of various challenges in camera based HSI analysis. Khan et al. [14] used fuzzy c-means clustering and k-fold cross validation for improved ink discrimination results. However, the non-practical assumption of two equal inks in a forged document make these methods unsuitable for practical situations where a small part of the document is manipulated. Abbas et al. [15] deliberated on hyperspectral unmixing and subspace identification for differentiating different inks present in varying mixing ratios in a document. Hyperspectral Subspace Identification by Minimum Error (HySime) algorithm is employed to determine and overestimate the number of inks in a questioned document, which is then reduced by weighted affine set fitting. Minimum Volume Enclosing Simplex (MVES) technique is used for unmixing on the basis of estimated number of inks for ink mismatch detection [15]. Luo et al. [11] focused on the minor variations in the quality or standard of ink in fraudulent and authentic documents based on localized hyperspectral image analysis and unsupervised learning. Khan et al. [16] employed CNN for ink classification based on spectral reflectance of text pixels for document forgery detection. A suitable architecture was experimentally selected and a significant improvement in ink discrimination results was observed.

B. *HSI Classification using Spatio-Spectral Hybrid Features*

The spatial resolution in a HSI measures the inter-pixel geometrical relation, while the spectral resolution estimates the intra-pixel variations in several narrowly spaced and contiguous channels in the infrared, near-infrared and visible segments. This exhibits great potential for precise discrimination between materials on the basis of distinctive spectral response of each material [26]. The trend towards using multiple features, such as spatio-spectral hybrid features is increasing because it significantly improves the image classification accuracy [27]. Pixel classification is typically used in HSI analysis [17], however, HSIs are spectrally smooth, i.e. the spectra of neighboring pixels are eminently inter-correlated, due to which spatio-spectral hybrid features yield improved HSI classification results [12]. Hyperspectral data is organized such that both spatial and spectral features can be exploited without any significant increase in computational cost. Akhtar et al. [28] have proposed a spatio-spectral framework for estimation of super-resolution HSI, in which spectral responses from low spectral resolution HSI are fused with a sparse code generated on the basis of sparsity, spatial properties and non-negativity of the scene in G-SOMP+ algorithm. Khan et al. [29] have collected a multi-illuminant HSI database and proposed an adaptive spatio-spectral hybrid approach for spectral reflectance recovery which is essential in analysis of HSIs. Shu et al. [30] have used Principal Component Analysis (PCA) and K-means clustering to learn spatial features which are concatenated in spectral bands to generate spatio–spectral feature representations for classification. Han et al. [31] presented a two-stream convolutional architecture for HSI classification that learns rich spatio-spectral features at different scales by performing row-column transformation and spatial rotation prior to feature extraction.

C. *Feature Extraction and Dimensionality Reduction in HSI*

Feature extraction in HSIs is challenging due to the spatial variations of spectral responses [32]. Hyperspectral data is naturally non-linear because of the complex light scattering mechanisms of natural objects. Therefore, linear transformation based feature extraction techniques are not directly applicable to hyperspectral data. Kernel based algorithms and manifold learning techniques offer a possibility to extract features from hyperspectral data but these methods use only 1-2 layers of processing such as linear SVM, logistic regression, PCA, kernel based SVM and decision tree. The human visual system naturally processes the information at different levels due to which multilayer systems are more biologically plausible for image classification tasks [33]. Modern deep learning techniques, such as stacked autoencoder [10], sparse autoencoder [34] and deep belief network [35] extract features using multiple layers which results in better image classification results.

The deep learning methods discussed above include a lot of train parameters because they exhibit full connection between adjacent layers. However, it is not needed in the case of small amounts of training data and also requires representation of spatial data in a vector form which may not efficiently extract the spatial features. CNN is the most commonly used deep learning method for automatic feature extraction and image classification [36]. The spectral response vectors are reshaped into image and directly passed to CNN model for feature extraction and pixel classification. Better descriptive features are extracted if both the spatial and the spectral information are taken into account [12]. Spectral information of the neighboring pixels combined for classification of a single pixel highly increases the dimensionality which is reduced by decreased training parameters and weight sharing in CNN. Moreover, regularization methods such as dropout and activation methods such as rectified linear unit help to avoid over-fitting and generalize the CNN model [37].

III. Proposed Method

We propose a deep learning based ink mismatch detection method for HSDIs that employs a combination of spectral and spatial features for classification of ink pixels. The database, pre-processing, spatio-spectral data formats and CNN based classification model are discussed in the following subsections.

A. *Database and Pre-processing*

The WIHSI database [7] contains fourteen hyperspectral images with 752 x 480 pixels, each with 33 spectral bands in the spectral range of 400~720nm. The images have non-uniform illumination, therefore Sauvola's local thresholding [38] is used to segment text pixels. A single document in the dataset contains five lines of an English phrase written with five distinct types of ink of either black or blue color by one of the seven subjects. All inks belong to different pen brands, so there are minor variations within same-colored inks. Each hyperspectral image is decomposed into five parts to generate a database of seventy hyperspectral images, each having one line written with one type of ink by one subject.

B. *Hyperspectral Mixing of Ink Samples*

The primary goal of HSI based ink analysis is to differentiate between visually similar but spectrally unique inks. In order to test the proposed algorithm in different scenarios, portions of the hyperspectral images of distinct ink samples with the same color and written by the same subject are merged in different ratios to produce different combinations of inks. Specifically, five different inks of the same color are mixed in pairs of 2, 3, 4 and 5 in the ratios of 1:1, 1:2, 1:4, 1:8, 1:16, 1:32, 1:1:1, 1:1:1:1 and 1:1:1:1:1. Blue and black ink samples were not inter-mixed because they can be easily differentiated by color imaging or visual analysis. Samples of different subjects are also not inter-mixed because identification of subject is not intended, only identification of ink type for ink mismatch detection is intended. The ground truth of these mixed hyperspectral images is kept to measure the performance of the proposed ink mismatch detection system during experimentation.

TABLE I. Six CNN Architectures Compared For Selection Of Suitable Architecture For Document Authentication

I	II	**III**	IV	V	VI
		Layers			
InputLayer	InputLayer	**InputLayer**	InputLayer	InputLayer	InputLayer
Conv1(3x3, 6)	Conv1(5x5, 6)	**Conv1(3x3, 6)**	Conv1(5x5, 6)	Conv1(3x3, 6)	Conv1(5x5, 6)
ReLU-Layer	ReLU-Layer	**ReLU-Layer**	ReLU-Layer	ReLU-Layer	ReLU-Layer
Conv2(3x3, 18)	Conv2(5x5, 18)	**Conv2(3x3, 18)**	Conv2(5x5, 18)	Conv2(3x3, 18)	Conv2(5x5, 18)
ReLU-Layer	ReLU-Layer	**ReLU-Layer**	ReLU-Layer	ReLU-Layer	ReLU-Layer
MaxPool1(2x2)	MaxPool1(2x2)	**MaxPool1(2x2)**	MaxPool1(2x2)	MaxPool1(2x2)	MaxPool1(2x2)
DropoutLayer(0.5)	DropoutLayer(0.5)	**Conv3(3x3, 36)**	Conv3(5x5, 36)	Conv3(3x3, 36)	Conv3(5x5, 6)
FullyConnected(5)	FullyConnected(5)	**ReLU-Layer**	ReLU-Layer	ReLU-Layer	ReLU-Layer
Softmax Layer	Softmax Layer	**Conv4(3x3, 54)**	Conv4(5x5, 54)	Conv4(3x3, 54)	Conv4(5x5, 18)
		ReLU-Layer	ReLU-Layer	ReLU-Layer	ReLU-Layer
		MaxPool2(2x2)	MaxPool2(2x2)	MaxPool2(2x2)	MaxPool2(2x2)
		DropoutLayer(0.5)	DropoutLayer(0.5)	Conv5(3x3, 72)	Conv5(5x5, 72)
		FullyConnected(5)	FullyConnected(5)	ReLU-Layer	ReLU-Layer
		Softmax Layer	Softmax Layer	Conv6(3x3, 90)	Conv6(5x5, 90)
				ReLU-Layer	ReLU-Layer
				MaxPool3(2x2)	MaxPool3(2x2)
				DropoutLayer(0.5)	DropoutLayer(0.5)
				FullyConnected(5)	FullyConnected(5)
				Softmax Layer	Softmax Layer
		Total No. of Training Parameters			
2,346	4,188	**37,500**	80,796	163,464	372,648
		Average Accuracy using 8-neighborhood (Blue, Black)			
(98.5, 88.3)	(97.4, 86)	**(99.6, 92.3)**	(98.8, 89.2)	(67.4, 62)	(61, 53.7)

C. Spectral-Spatial Data Organization

The spectral responses of a target pixel and its neighboring pixels are formatted in an image form. The 'target pixel' is the pixel intended for classification. Three different spatio-spectral strategies are used: an ink pixel is classified on the basis of the spectral response of (i) the target pixel only, (ii) the target pixel and its 4-neighbors, (iii) the target pixel and its 8-neighbors. These three spatio-spectral strategies are illustrated in Figure 1(a-c). To make the combined spectral and spatial information of ink pixels compatible with the CNN, the spectral responses of pixels are organized into one 2D image. Figure 1(d-f) shows a single image format designed for each spatio-spectral strategy. The alternating light brown and dark brown pixels show the places for spectral responses of the pixels numerically labelled in Figure 1(a-c), whereas the light gray pixels represent zero values. The number of nodes in the input layer of each CNN architecture is modified for each of these three data formats, without making any changes to the hidden layers.

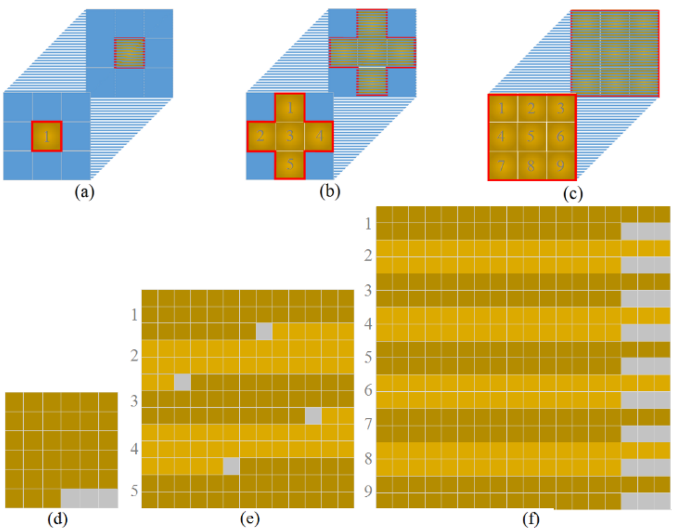

Fig. 1. Three spatio-spectral strategies adopted for classification of the target pixel with (a) no neighbouring pixels, (b) 4-neighbors and (c) 8-neighbors, and their three corresponding image formats for organizing the target and the neighbouring pixels in a single image of size (d) 6x6, (e) 13x13 and (f) 18x18.

TABLE II. ORGANIZATION OF SPECTRAL RESPONSES

Ink Color	**No. of Ink Types**	**Training Ratio**	**No. of spectral response samples**		
			Training	*Testing*	*Total*
Black	5	6:1	94,971	14,718	109,689
		5:2	81,881	27,808	
		4:3	67,186	42,503	
		3:4	42,503	67,186	
		2:5	27,808	81,881	
		1:6	14,718	94,971	
Blue	5	6:1	83,407	13,075	96,482
		5:2	70,975	25,507	
		4:3	58,235	38.247	
		3:4	38,247	58,235	
		2:5	25,507	70,975	
		1:6	13,075	83,407	
Total	10	-	-	-	206,171

D. CNN Architecture & Training Process

We implemented six different CNN architectures, presented in Table I. The spectral responses of ink pixels in all hyperspectral images are extracted and used to train and test the CNN in different ratios, in terms of subjects, as shown in Table II. Training ratio 6:1 means that the spectral responses of ink pixels corresponding to six subjects are used to train the CNN and that of one subject are used for testing. The performance is evaluated for all training ratios. The selection of appropriate layered architecture, training ratio and hyperparameters aids the CNN in learning suitable features.

E. CNN Classification

A trained CNN, explained in the previous section, is used for classification of ink pixels for ink discrimination and detection of ink mismatch in an input HSDI after the preprocessing steps. Classified ink pixels are color labelled for visual inspection and authentication the document under examination.

IV. EXPERIMENTS AND RESULTS

The experiments were conducted on a GPU enabled workstation with 18-cores and 64-bit Intel 2.3GHz processor, 64GB RAM and GPU with a compute capability of 3.5 and 12GB memory. The six CNN models, presented in Table I, were trained on spectral responses of inks organized in the three different image formats shown in Figure 1 and using different training ratios as shown in Table II. The accuracy achieved by each CNN architecture using each image format in presented in Figure 2. Due to the small input image sizes of 6x6, 13x13 and 18x18, the CNN models with smaller filters (3x3) achieved higher accuracy as compared to the larger filters (5x5).

In CNN architectures, adding more layers helps in extracting more features that generally improves the accuracy up to a certain extent after which further increasing the layers tends to overfit the model. Figure 2 shows that architecture I and II achieve a high accuracy, which is further improved by increasing the number of layers in architecture III and IV. Further increasing the number of layers in architecture V and VI results in lower accuracies due to overfitting. It is also observed that using fewer filters in starting layers and increasing them in later layers improves the performance. Hence CNN-III is chosen for further experiments as the most suitable architecture for ink mismatch detection. It is noted that comparatively higher accuracy is achieved on the blue inks as compared to the black inks in all cases. This is because the spectral responses of the black inks are confined into a narrower reflectance range as compared to the blue inks which makes it easier to discriminate between the blue inks, as shown in Figure 3.

The performance of CNN-III with different training ratios is presented in Figure 4, which shows that CNN-III achieves the highest accuracy when the training ratio is maximum, i.e. 6:1. The accuracy decreases as the number of training samples decreases as compared to the number of testing samples. The CNN Architecture-III used with 8-neighbors spatio-spectral format and training ratio of 6:1 stands out as the most suitable

CNN architecture, which is used for further testing on the mixed ink combinations. Average accuracies of 99.6% for blue and 92.3% for black inks are observed, which are the highest accuracy measures achieved in ink discrimination on the WIHSI database so far. A detailed comparison of the proposed method employing CNN-III with 8-neighbors spatio-spectral format and training ratio of 6:1, with the previous methods on this subject using the WIHSI database is summarized in Table III. The proposed method outperforms the previous methods by achieving the highest accuracy on the mixed ink combinations with unbalanced proportions.

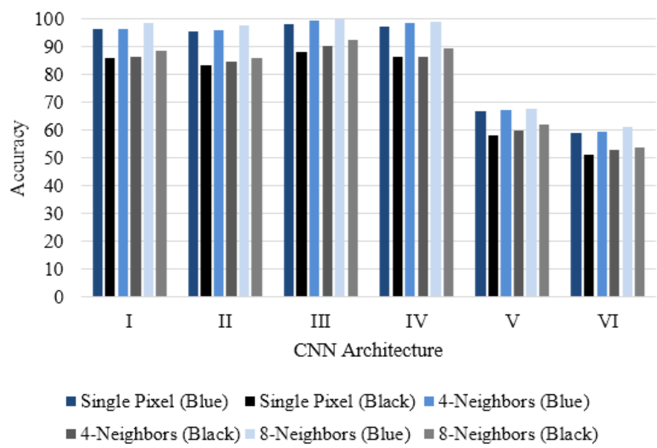

Fig. 2. Accuracy of all CNN models using three different spatio-spectral data formats (presented in Fig. 1).

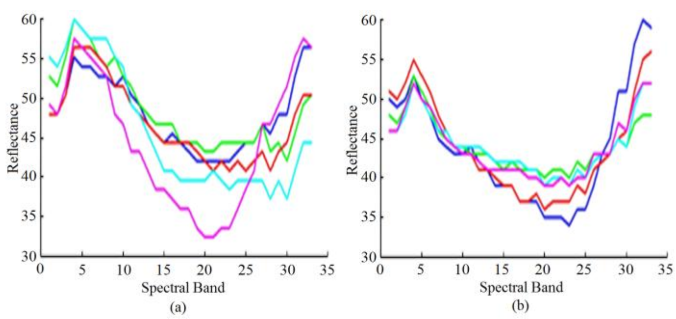

Fig. 3. Spectral responses of (a) each blue ink type and (b) each black ink, showing that blue inks are easily distinguishable as compared to the black inks in the UWA WIHSI database.

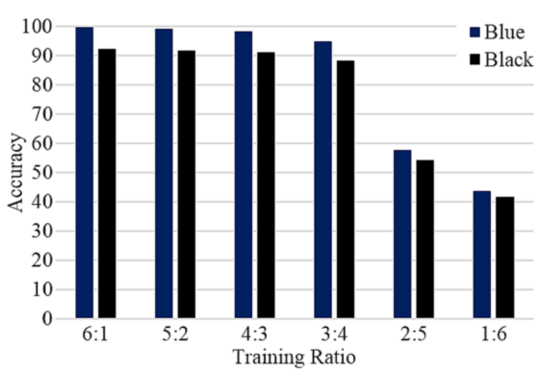

Fig. 4. Performance of CNN-III with different training ratios

V. Conclusion and Future Prospects

A robust and accurate ink mismatch detection system is essential for authentication of questioned documents. We have proposed a CNN based document authentication method for hyperspectral document images, in which we exploit the spectral correlation as well as the spatial context to enhance ink classification. Comprehensive experiments are performed on mixed ink combinations containing inks from different manufacturers mixed in varying ratios and promising results are obtained which outclass the previous methods on this subject. Apart from selecting an appropriate architecture and training parameters of CNN, the most suitable ratio of training and testing samples is also selected experimentally. The proposed method requires prior knowledge for training, due to which, its practical applicability is limited to situations in which prior knowledge of ink types present in the questioned documents is readily available. However, this limitation can be overcome by employing unsupervised deep learning in the future work. Moreover, the proposed method can be altered for its use in identification of subjects on spatio-spectral hybrid features of text, which could be a new aspect for document authentication.

TABLE III. Summary of Comparative Study with Previous Methods

Method	**Accuracy (%)**		**Maximum Inks per Document**	**Uneven amounts of ink**	**Type of Information Used**
	Blue	*Black*			
Proposed Method	99.6	92.3	5	Yes	Spatial and Spectral
Khan et al. [16]	98.2	88.0	5	Yes	Spectral Only
Abbas et al. [15]	86.2	83.4	4	Yes	Spectral Only
Luo et al. [13]	89.0	82.3	2	Yes	Spectral Only
Khan et al. [14]	86.7	81.9	2	No	Spectral Only
Khan et al. [7]	85.6	81.4	2	No	Spectral Only

References

[1] M. J. Khan, H. S. Khan, A. Yousaf, K. Khurshid, and A. Abbas, “Modern Trends in Hyperspectral Image Analysis: A Review,” *IEEE Access*, vol. 6, no. 1, pp. 14118–14129, 2018.

[2] G. J. Edelman, E. Gaston, T. G. van Leeuwen, P. J. Cullen, and M. C. G. Aalders, “Hyperspectral imaging for non-contact analysis of forensic traces,” *Forensic Sci. Int.*, vol. 223, no. 1–3, pp. 28–39, Nov. 2012.

[3] R. L. Easton, K. T. Knox, and W. A. Christens-Barry, “Multispectral imaging of the archimedes palimpsest,” in *32nd Applied Imagery Pattern Recognition Workshop, 2003. Proceedings.*, pp. 111–116.

[4] W. A. Christens-Barry, K. Boydston, F. G. France, K. T. Knox, R. L. Easton, Jr., and M. B. Toth, “Camera system for multispectral imaging of documents,” 2009, vol. 7249, p. 724908.

[5] C. Balas, V. Papadakis, N. Papadakis, A. Papadakis, E. Vazgiouraki, and G. Themelis, “A novel hyper-spectral imaging apparatus for the non-destructive analysis of objects of artistic and historic value,” *J. Cult. Herit.*, vol. 4, pp. 330–337, Jan. 2003.

[6] K. Melessanaki, V. Papadakis, C. Balas, and D. Anglos, “Laser induced breakdown spectroscopy and hyper-spectral imaging analysis of pigments on an illuminated manuscript,” *Spectrochim. Acta Part B At. Spectrosc.*, vol. 56, no. 12, pp. 2337–2346, Dec. 2001.

[7] Z. Khan, F. Shafait, and A. Mian, “Hyperspectral Imaging for Ink Mismatch Detection,” in *2013 12th International Conference on*

Document Analysis and Recognition, 2013, pp. 877–881.

[8] S. Joo Kim, F. Deng, and M. S. Brown, “Visual enhancement of old documents with hyperspectral imaging,” *Pattern Recognit.*, vol. 44, no. 7, pp. 1461–1469, Jul. 2011.

[9] K. Iqbal and K. Khurshid, “Automatic Signature Extraction from Document Images using Hyperspectral Unmixing,” *Proc. Pakistan Acad. Sci.*, vol. 54, no. 3, pp. 257–265, 2017.

[10] Y. Chen, Z. Lin, X. Zhao, G. Wang, and Y. Gu, “Deep Learning-Based Classification of Hyperspectral Data,” *IEEE J. Sel. Top. Appl. Earth Obs. Remote Sens.*, vol. 7, no. 6, pp. 2094–2107, Jun. 2014.

[11] H. Liang and Q. Li, “Hyperspectral Imagery Classification Using Sparse Representations of Convolutional Neural Network Features,” *Remote Sens.*, vol. 8, no. 2, p. 99, Jan. 2016.

[12] J. Leng, T. Li, G. Bai, Q. Dong, and H. Dong, “Cube-CNN-SVM: A Novel Hyperspectral Image Classification Method,” in *2016 IEEE 28th International Conference on Tools with Artificial Intelligence (ICTAI)*, 2016, pp. 1027–1034.

[13] Z. Luo, F. Shafait, and A. Mian, “Localized forgery detection in hyperspectral document images,” in *2015 13th International Conference on Document Analysis and Recognition (ICDAR)*, 2015, pp. 496–500.

[14] M. J. Khan, A. Yousaf, K. Khurshid, A. Abbas, and F. Shafait, “Automated Forgery Detection in Multispectral Document Images using Fuzzy Clustering,” in *13th IAPR International Workshop on Document Analysis Systems*, 2018.

[15] A. Abbas, K. Khurshid, and F. Shafait, “Towards Automated Ink Mismatch Detection in Hyperspectral Document Images,” in *2017 14th IAPR International Conference on Document Analysis and Recognition (ICDAR)*, 2017, pp. 1229–1236.

[16] M. J. Khan, A. Yousaf, A. Abbas, and K. Khurshid, “Deep learning for automated forgery detection in hyperspectral document images,” *J. Electron. Imaging*, vol. 27, no. 05, p. 1, Sep. 2018.

[17] J. M. Bioucas-Dias, A. Plaza, G. Camps-Valls, P. Scheunders, N. Nasrabadi, and J. Chanussot, “Hyperspectral Remote Sensing Data Analysis and Future Challenges,” *IEEE Geosci. Remote Sens. Mag.*, vol. 1, no. 2, pp. 6–36, Jun. 2013.

[18] E. B. Brauns and R. B. Dyer, “Fourier Transform Hyperspectral Visible Imaging and the Nondestructive Analysis of Potentially Fraudulent Documents,” *Appl. Spectrosc.*, vol. 60, no. 8, pp. 833–840, Aug. 2006.

[19] R. Padoan, T. Steemers, M. Klein, B. Aalderink, and G. De Bruin, “Quantitative hyperspectral imaging of historical documents: technique and applications,” in *ART Proceedings*, 2008.

[20] K. Franke and S. Rose, “Ink-Deposition Model: The Relation of Writing and Ink Deposition Processes,” in *Ninth International Workshop on Frontiers in Handwriting Recognition*, pp. 173–178.

[21] K. Franke, O. Bunnemeyer, and T. Sy, “Ink texture analysis for writer identification,” in *Proceedings Eighth International Workshop on Frontiers in Handwriting Recognition*, 2002, pp. 268–273.

[22] C. S. Silva, M. F. Pimentel, R. S. Honorato, C. Pasquini, J. M. Prats-Montalbán, and A. Ferrer, “Near infrared hyperspectral imaging for forensic analysis of document forgery,” *Analyst*, vol. 139, no. 20, pp. 5176–5184, Jul. 2014.

[23] A. Morales, M. A. Ferrer, M. Diaz-Cabrera, C. Carmona, and G. L. Thomas, “The use of hyperspectral analysis for ink identification in handwritten documents,” in *2014 International Carnahan Conference on Security Technology (ICCST)*, 2014, pp. 1–5.

[24] R. Qureshi, M. Uzair, K. Khurshid, and H. Yan, “Hyperspectral document image processing: Applications, challenges and future prospects,” *Pattern Recognit.*, vol. 90, pp. 12–22, Jun. 2019.

[25] Z. Khan, F. Shafait, and A. Mian, “Automatic ink mismatch detection for forensic document analysis,” *Pattern Recognit.*, vol. 48, no. 11, pp. 3615–3626, Nov. 2015.

[26] D. Landgrebe, “Information Extraction Principles and methods for multispectral and hyperspectral image data,” in *Information Processing For Remote Sensing*, World Scientific, 1999, pp. 3–37.

[27] C. Zhao, X. Gao, Y. Wang, and J. Li, “Efficient Multiple-Feature Learning-Based Hyperspectral Image Classification With Limited Training Samples,” *IEEE Trans. Geosci. Remote Sens.*, vol. 54, no. 7, pp. 4052–4062, Jul. 2016.

[28] N. Akhtar, F. Shafait, and A. Mian, “Sparse Spatio-spectral Representation for Hyperspectral Image Super-resolution,” in *European Conference on Computer Vision (ECCV)*, 2014, pp. 63–78.

[29] Z. Khan, F. Shafait, and A. Mian, “Adaptive spectral reflectance recovery using spatio-spectral support from hyperspectral images,” in *2014 IEEE International Conference on Image Processing (ICIP)*, 2014, pp. 664–668.

[30] L. Shu, K. McIsaac, and G. R. Osinski, “Learning Spatial–Spectral Features for Hyperspectral Image Classification,” *IEEE Trans. Geosci. Remote Sens.*, vol. 56, no. 9, pp. 5138–5147, Sep. 2018.

[31] M. Han, R. Cong, X. Li, H. Fu, and J. Lei, “Joint spatial-spectral hyperspectral image classification based on convolutional neural network,” *Pattern Recognit. Lett.*, Oct. 2018.

[32] X. Jia, B.-C. Kuo, and M. M. Crawford, “Feature Mining for Hyperspectral Image Classification,” *Proc. IEEE*, vol. 101, no. 3, pp. 676–697, Mar. 2013.

[33] N. Kruger *et al.*, “Deep Hierarchies in the Primate Visual Cortex: What Can We Learn for Computer Vision?,” *IEEE Trans. Pattern Anal. Mach. Intell.*, vol. 35, no. 8, pp. 1847–1871, Aug. 2013.

[34] Chao Tao, Hongbo Pan, Yansheng Li, and Zhengrou Zou, “Unsupervised Spectral–Spatial Feature Learning With Stacked Sparse Autoencoder for Hyperspectral Imagery Classification,” *IEEE Geosci. Remote Sens. Lett.*, vol. 12, no. 12, pp. 2438–2442, Dec. 2015.

[35] Y. Chen, X. Zhao, and X. Jia, “Spectral–Spatial Classification of Hyperspectral Data Based on Deep Belief Network,” *IEEE J. Sel. Top. Appl. Earth Obs. Remote Sens.*, vol. 8, no. 6, pp. 2381–2392, Jun. 2015.

[36] A. Krizhevsky, I. Sutskever, and G. E. Hinton, “ImageNet Classification with Deep Convolutional Neural Networks.” pp. 1097–1105, 2012.

[37] Y. Chen, H. Jiang, C. Li, X. Jia, and P. Ghamisi, “Deep Feature Extraction and Classification of Hyperspectral Images Based on Convolutional Neural Networks,” *IEEE Trans. Geosci. Remote Sens.*, vol. 54, no. 10, pp. 6232–6251, Oct. 2016.

[38] F. Shafait, D. Keysers, and T. M. Breuel, “Efficient implementation of local adaptive thresholding techniques using integral images,” in *Document Recognition and Retrieval XV*, 2008, vol. 6815, pp. 681510-681510–6.